ELSEVIER

Steroids 64 (1999) 385–395

Steroids

An improved synthesis of (20*R*,22*R*)-cholest-5-ene-3β,20,22-triol, an intermediate in steroid hormone formation and an activator of nuclear orphan receptor LXRα

Benfang Ruan[a], William K. Wilson[b], George J. Schroepfer Jr.[a,b,*]

[a]*Department of Chemistry, Rice University, Houston, Texas 77005, USA*
[b]*Department of Biochemistry and Cell Biology, Rice University, Houston, Texas 77005, USA*

Received 31 August 1998; accepted 27 October 1998

Abstract

Asymmetric dihydroxylation of (20(22)*E*)-cholesta-5,20(22)-dien-3β-ol acetate (**2a**), prepared from pregnenolone, gave a 1:1 mixture (67% yield) of (20*R*,22*R*)-cholest-5-ene-3β,20,22-triol 3-acetate (**3a**) and its 20*S*,22*S* isomer **3b**. Highly purified **3a** and **3b** were obtained by semipreparative silver ion high performance liquid chromatography. Saponification of **3a** and **3b** gave (20*R*,22*R*)-cholest-5-ene-3β,20,22-triol (**4a**) and its 20*S*,22*S* isomer **4b**. This simple approach provided the natural isomer **4a** more efficiently than previously described chemical or enzymatic syntheses. Full ^{1}H and ^{13}C nuclear magnetic resonance data were presented for triols **4a** and **4b** and their synthetic precursors. Side-chain conformations of **2a**, its 20(22)Z isomer, **4a**, and **4b** were studied by molecular mechanics and nuclear Overhauser effect difference spectroscopy.

Keywords: (20*R*,22*R*)-Cholest-5-ene-3β,20,22-triol; Asymmetric dihydroxylation; AD-mix; Ag^{+}-HPLC; NMR; Molecular mechanics; Conformational analysis

1. Introduction

(20*R*,22*R*)-Cholest-5-ene-3β,20,22-triol [(20*R*,22*R*)-20,22-dihydroxycholesterol; **4a**] is an intermediate in the enzymatic conversion of cholesterol to pregnenolone and other steroid hormones [1–3] and has been reported to be present in bovine adrenal glands at a level of 2.15 μg/g [4]. The 20,22-dihydroxysterol **4a** has also recently been reported to activate the nuclear orphan receptor LXRα [5,6]; the 20*R*,22*R* isomer **4a** was found to be considerably more potent than the 20*S*,22*S* isomer **4b**, albeit less potent than (20*S*)-20-hydroxycholesterol [6]. Despite its important biological roles, **4a** is not commercially available, a situation that prompted its recent preparation in 9.6% yield (240 μg) by 'large-scale' incubation of (22*R*)-22-hydroxycholesterol with placental mitochondria [7]. Previous chemical syntheses of **4a** were either lengthy or gave the desired isomer in a low yield [8–12]. Described herein is an improved synthesis of the 20*R*,22*R* isomer **4a**. A preliminary account of a portion of this work has already been presented [6].

2. Experimental procedures and results

2.1. General methods and materials

Melting points (mp) were measured in sealed, evacuated capillary tubes by using a Thomas-Hoover apparatus (Thomas Scientific; Swedesboro, NJ, USA). Thin-layer chromatography (TLC) was carried out by using aluminum-backed silica gel 60 plates (EM Science, Gibbstown, NJ, USA). Components on the plates were visualized after spraying with 5% ammonium molybdate in 10% sulfuric acid and heating. Silica gel (230–400 mesh) was used for routine column chromatography and for medium pressure liquid chromatography (MPLC). For MPLC, fractions (20 ml) were collected every 5 min and analyzed by TLC. Normal phase high performance liquid chromatography (HPLC) was carried out on an Adsorbosphere silica column

* Corresponding author. Department of Biochemistry and Cell Biology, MS 140, Rice University, 6100 Main St., Houston, Texas 77005-1892. Tel: +1-713-527-4914; fax: +1-713-285-5154. Deceased 11 December, 1998.

0039-128X/99/$ – see front matter
PII: S0039-128X(98)00116-0

(250 × 4.6 mm) obtained from Alltech Associates (Deerfield, IL, USA). Ag^+-HPLC was carried out with 5 μm Nucleosil SA columns (250 × 4.6 mm, 300 × 3.2 mm, or 300 × 10 mm), which were obtained from Alltech Associates, charged with silver ion, and prepared for use as described previously [13,14]. Flow rates for analytical and semipreparative columns were 1 ml/min and 3 ml/min, respectively. Elution of the sterols and steryl acetates from the HPLC columns, using mixtures of acetone and hexane, was monitored by ultraviolet (UV) absorbance at 210 nm. Capillary gas chromatography (GC) was carried out on a Shimadzu GC-9A instrument (Shimadzu Scientific Instruments; Columbia, MD, USA) with a 30-m DB-5 column (injector temperature, 200°C; column temperature, 60°C for 5 min followed by a temperature increase of 10°C/min to 200°C, and thereafter maintained at 200°C for 5 min). Nitrogen was used as the carrier gas with a head pressure of 1.1 kg/cm^2. Mass spectra (MS) were recorded on a VG ZAB-HF double sector instrument (Micromass; Manchester, UK) with an electron energy of 70 eV and direct inlet sample introduction. Unless stated otherwise, GC-MS was carried out on the same instrument coupled to an HP-5890A GC unit containing a 60-m DB-5 column (0.25 mm ID; 0.1 μm film thickness; J & W Scientific Inc., Folsom, CA, USA). The column temperature was 250°C, and the temperatures of the injector and GC-MS interface were 290°C. Helium was used as the carrier gas, with a head pressure of 1.4 kg/cm^2. Trimethylsilyl (TMS) derivatives of the sterols were prepared by treatment with a 1:1 mixture of *N,O*-bis(trimethylsilyl)trifluoroacetamide and pyridine at 50°C for 2 h. Nuclear magnetic resonance (NMR) spectra were recorded as described previously [15] on a Bruker AMX500 (Bruker Instruments, Billerica, MA; USA) spectrometer [5–15 mM $CDCl_3$ solution at 25°C for ^{1}H; 10–80 mM $CDCl_3$ solution at 22°C for ^{13}C) and referenced to an internal standard of tetramethylsilane (^{1}H) or $CDCl_3$ at 77.0 ppm (^{13}C). Signal assignments were made from heteronuclear single-quantum coherence (HSQC), COSYDEC (f_1-decoupled ^{1}H-^{1}H correlation spectroscopy), COSY-DQF (^{1}H-^{1}H correlation spectroscopy with double-quantum filtering), DEPT (distortionless enhancement by polarization transfer), NOE (nuclear Overhauser effect) difference, and 1D spectra as described previously [15]. Coupling constants were measured from resolution-enhanced 1D spectra or at lower precision from coupled [16] or decoupled HSQC spectra (linear predicted in f_2 to 4k points). Chemical shifts were corrected for strong coupling in 1D spectra by analogy with the analysis of AB spin systems and in COSYDEC spectra by using corrections based on spectral simulations with NMR-SIM (Bruker Instruments). PCMODEL 7.0 (Serena Software; Bloomington, IN, USA) was used for modeling of sterol structures by molecular mechanics and for predicting vicinal ^{1}H-^{1}H NMR-coupling constants. Molecular mechanics was also done with MM3 (94) from the Quantum Chemistry Program Exchange (Bloomington, IN, USA) and an implementation of MM2 in Chem3D Pro 3.5 (Cambridge Soft; Cambridge, MA, USA).

The following compounds were obtained from Aldrich Chemical Company (Milwaukee, WI, USA): 4-methyl-1-pentanol, methyltriphenoxyphosphonium iodide, triphenylphosphine, sodium *tert*-amylate, methanesulfonamide, AD-mix-α, and AD-mix β. The AD-mix reagents [17] contain $K_3Fe(CN)_6$, K_2CO_3, $K_2OsO_4 \cdot 2H_2O$, and either hydroquinine 1,4-phthalazinediyl diether [$(DHQD)_2$PHAL] (AD-mix-α) or hydroquinidine 1,4-phthalazinediyl diether [$(DHQ)_2$PHAL] (AD-mix-β). 3β-Hydroxypregn-5-en-20-one (pregnenolone) was purchased from Sigma (St. Louis, MO, USA). 1-Iodo-4-methylpentane (isohexyl iodide) was prepared from 4-methyl-1-pentanol by an adaptation of the method of Rydon [18] by stirring a mixture of methyltriphenoxyphosphonium iodide (50 g; 110.6 mmol) and 4-methyl-1-pentanol (13.8 ml; 111 mmol) at room temperature for 24 h. Capillary GC of the reaction mixture (overloaded) showed a major component at retention time (t_R) 5.0 min (91%) and minor components at t_R 1.4 min (3%) and t_R 2.4 min (4%) corresponding to methyl iodide (t_R 1.4 min) and 4-methyl-1-pentanol (t_R 2.4 min). Vacuum distillation over a 13-cm Vigreux column gave isohexyl iodide (boiling point 27°C, 0.1 torr): boiling point ~165°C (760 torr); GC-MS (Extrel ELQ-400; ABB Extrel; Pittsburgh, PA, USA), *m/z* 212 (100, M^+), 127 (60, I). Isohexyltriphenylphosphonium iodide was prepared by an adaptation of conditions reported by Schow and McMorris [19] for the preparation of another alkyltriphenylphosphonium halide by adding triphenylphosphine (27 g; 104 mmol) to a solution of isohexyl iodide (22 g; 104 mmol) in toluene (20 ml) and refluxing the resulting mixture for 24 h under argon. GC analysis of the reaction mixture showed an almost complete disappearance of the isohexyl iodide (t_R 5.0 min). The white solid that precipitated upon cooling to room temperature was collected, washed with anhydrous ether (3 × 300 ml), and dried under vacuum to give isohexyltriphenylphosphonium iodide (48.6 g): ^{1}H NMR, δ 7.83 (m, 9H), 7.72 (m, 6H), 3.69 (m, 2H), 1.64 (m, 2H), 1.53 (m, 3H), and 0.80 (d, 6.3 Hz, 6H).

2.2. (20(22)E)-Cholesta-5,20(22)-dien-3β-ol **(1)**

Compound **1** was prepared by modifications of the methods of Schmit et al. [20] and Schow and McMorris [19]. To isohexyltriphenylphosphonium iodide (1.6 g; 3.5 mmol) was added benzene (4 ml) and potassium *tert*-butoxide (3.5 mmol) in *tert*-butanol (3.5 ml). This mixture was heated under reflux for 30 min under argon and then cooled to room temperature. The solvent was removed under reduced pressure under argon, and the resulting residue was dissolved in benzene (6 ml). To the resulting red solution was quickly added pregnenolone (126 mg; 0.4 mmol) in hot benzene (4 ml), and the mixture was heated under reflux for 2 h. After the reaction was complete (as judged by TLC; solvent 25% acetone in hexane), the solution was cooled to

Table 1
^{1}H NMR chemical shifts of 3β,20,22-triols and their synthetic precursors[a–c]

	17β-C_8H_{15} $\Delta^{5,20(22)E}$ 3β-OH **1**	17β-C_8H_{15} $\Delta^{5,20(22)E}$ 3β-OAc **2a**	17β-C_8H_{15} $\Delta^{5,20(22)Z}$ 3β-OAc **2b**	17α-C_8H_{15} $\Delta^{5,20(22)E}$ 3β-OAc **2c**	20*R*,22*R* Δ^5 3β-OAc **3a**	20*S*,22*S* Δ^5 3β-OAc **3b**	20*R*,22*R* Δ^5 3β-OH **4a**	20*S*,22*S* Δ^5 3β-OH **4b**
H-1α	1.085	1.138	1.141	1.116†	1.131	1.138	1.076	1.086
H-1β	1.853†	1.864†	1.864†	1.85	1.862†	1.858†	1.849†	1.845†
H-2α	1.839†	1.861†	1.861†	1.85	1.861†	1.859†	1.84	1.838†
H-2β	1.501	1.587	1.588	1.580†	1.591	1.590	1.505	1.504
H-3α	3.528	4.607	4.610	4.60	4.606	4.604	3.530†	3.522†
H-4α	2.299	2.328†	2.333†	2.32	2.33	2.326†	2.300	2.297
H-4β	2.237	2.311†	2.311†	2.31	2.31	2.304†	2.238	2.234
H-6	5.358	5.380	5.387	5.379†	5.378	5.375	5.355	5.353
H-7α	1.549	1.557	1.582	1.589†	1.548	1.538	1.540†	1.531†
H-7β	1.994	1.990	2.003	2.01	1.979	1.976	1.983	1.979
H-8β	1.446	1.439	1.455	1.432†	1.483†	1.476	1.489†	1.484†
H-9α	0.958	0.977	0.989	0.885[d,†]	0.956	0.945	0.937	0.926
H-11α	1.549†	1.544†	1.539	1.52	1.533†	1.521†	1.538†	1.528†
H-11β	1.441†	1.434†	1.430	1.45	1.491†	1.492†	1.498†	1.495†
H-12α	1.175	1.185	1.160	1.108†	1.254	1.219	1.243	1.211
H-12β	1.799	1.797	1.689	1.52[d]	2.126	1.939	2.128	1.942
H-14α	1.064	1.073	1.107	0.943[d,†]	1.012	1.024	1.001	1.016†
H-15α	1.660†	1.660†	1.721	1.684†	1.639	1.650	1.638	1.650
H-15β	1.172	1.167	1.237	1.208†	1.156	1.158	1.160	1.162†
H-16α	1.607†	1.609†	1.594	1.60*[,d]	1.548†	1.757	1.550	1.755†
H-16β	1.809	1.807	1.868	1.956*[,†]	1.828	1.856	1.829	1.857†
H-17	1.998	2.001	2.530	2.211	1.500†	1.598	1.496	1.597
H-18	0.545	0.543	0.664	0.827	0.894	0.881	0.895	0.882
H-19	1.010	1.020	1.027	1.016	1.027	1.022	1.017	1.011
H-21	1.625	1.625	1.701	1.599	1.217	1.064	1.218	1.064
H-22	5.169	5.168	5.277	4.981	3.387†	3.728	3.388	3.728
H-23R	2.02	2.01*	1.929*	2.00	1.43	1.207†	1.43	1.20
H-23S	2.02	2.03*	2.099*	2.00	1.204†	1.55	1.204†	1.55
H-24R	1.22*	1.22*	1.18*	1.23	1.212†	1.572†	1.213†	1.57
H-24S	1.23*	1.24*	1.19*	1.23	1.455†	1.17	1.457†	1.18
H-25	1.554	1.554	1.539	1.56	1.556†	1.554†	1.556†	1.552†
H-26	0.884*	0.883*	0.868*	0.886*	0.897*	0.904*	0.898*	0.902*
H-27	0.886*	0.885*	0.880*	0.889*	0.909*	0.909*	0.910*	0.909*
Acetate		2.032	2.033	2.030	2.033	2.032		

[a] Data obtained at 500 MHz in 5–15 mM $CDCl_3$ solution at 25°C and referenced to $Si(CH_3)_4$. Chemical shifts given to two (three) decimal places are accurate to ± 0.01 (± 0.001) ppm except that values marked by † are accurate to ca. ± 0.003 ppm. Assignments of diastereotopic pairs marked with an asterisk (*) may be interchanged.

[b] Most coupling constants in the steroid nucleus and the side-chain terminus were similar to those of other Δ^5 sterols described in Ref. 15. Other coupling constants: H-17α, br dd ~10.5, 9 Hz (**1**, **2a**, **2b**), ddd, 9.1, 2.2, 0.6 Hz (**2c**), br dd, 10.3, 9.6 Hz (**3a**, **3b**, **4a**, **4b**); H-21, td, 1.1, 0.7 Hz (**1**, **2a**, **2b**), q, 1.4 Hz (**2c**), s (**3a**, **3b**, **4a**, **4b**); H-22, tt, 7.1, 1.3 Hz (**1**, **2a**, **2c**), dddd, 8.1, 6.1, 1.4, 0.6 Hz (**2b**), br dd, 9.2, ~2 Hz (**3b**, **4b**), ddd, ~10.2, 3.4, 1.7 Hz (**4a**); H-23*R*, br dddt, ~15, 8, 7, 1.5 Hz (**2b**), br tdd, ~12.5, 6, 2 Hz (**4a**); H-23*S*, br ddtd, ~15, 8, 7, 1.5 Hz (**2b**), br dtd, ~13, 11, 5 Hz (**4a**); H-24*R*, br ddt, ~13, 12, 6 Hz.

[c] Hydroxyl signals of **3a**, **3b**, **4a**, **4b** (variable): δ 2.3 (often dd, 3.4, 0.9 Hz, 22-OH), 1.9 (s, 20-OH), 1.6 (s).

[d] These and other chemical shifts for **2c** were extracted from low-resolution HSQC and COSYDEC spectra and are of some uncertainty.

room temperature, poured into water (30 ml), and extracted with ether (3 × 50 ml). The combined extracts were washed once with brine, dried over anhydrous sodium sulfate, and evaporated to dryness. The residue was subjected to silica gel MPLC (50 × 1 cm) using a mixture of 5% ethyl acetate in hexane as the eluting solvent. Fractions 15–28 were combined and evaporated to dryness to give a white solid (130 mg; 85%). GC analysis showed one major component (92%, t_R 25.2 min) and two minor components (2%, t_R 17.0 min; and 5.4%, t_R 21.2 min). A portion (50 mg) of this material was purified by Ag^+-HPLC (300 × 10 mm; 15% acetone in hexane) to give pure **1** (45 mg): single component (t_R 42.6 min) by GC-MS analysis of its TMS derivative, *m/z* 456 (100; M^+), 441 (12; M-CH_3), 366 (28; M-TMSOH), 351 (24; M-TMSOH-CH_3), 330 (9), 327 (8), 318 (8), 253 (10; M-SC-TMSOH), 228 (21), 213 (26), 156 (18), 145 (21), and 129 (55); ^{1}H NMR, Table 1; ^{13}C NMR, Table 2.

2.3. (20(22)E)-Cholesta-5,20(22)-dien-3β-ol acetate (2a)

Crude **1** (800 mg; 2.1 mmol; 92% purity) was treated with acetic anhydride (10 ml) and pyridine (10 ml) at room

Table 2
^{13}C NMR chemical shifts of 3β,20,22-triols and their synthetic precursors.[a]

	17β-C_8H_{15} $\Delta^{5,20(22)E}$ 3β-OH **1**	17β-C_8H_{15} $\Delta^{5,20(22)E}$ 3β-OAc **2a**	17β-C_8H_{15} $\Delta^{5,20(22)Z}$ 3β-OAc **2b**	17α-C_8H_{15} $\Delta^{5,20(22)E}$ 3β-OAc **2c**	20*R*,22*R* Δ^5 3β-OAc **3a**	20*S*,22*S* Δ^5 3β-OAc **3b**	20*R*,22*R* Δ^5 3β-OH **4a**	20*S*,22*S* Δ^5 3β-OH **4b**
C-1	37.25	36.99	37.01	37.00	36.96	36.97	37.21	37.24
C-2	31.63	27.74	27.75	27.76†	27.71	27.70	31.59	31.61
C-3	71.76	73.94	73.93	73.98	73.89	73.88	71.72	71.74
C-4	42.27	38.09	38.09	38.10	38.05	38.05	42.22	42.23
C-5	140.77	139.65	139.69	139.61	139.61	139.62	140.74	140.74
C-6	121.66	122.58	122.58	122.64	122.46	122.47	121.53	121.55
C-7	31.83	31.81	31.95	32.33††	31.70	31.73	31.72	31.75
C-8	32.16	32.12	31.87	32.29††	31.19	31.28	31.25	31.33
C-9	50.34	50.23	50.32	50.15**	49.92	49.80	50.01	49.91
C-10	36.55	36.63	36.70	36.62	36.53	36.57	36.46	36.49
C-11	21.05	20.99	20.71	20.98	20.86	20.88	20.92	20.95
C-12	38.62	38.56	38.18	34.60	40.10	40.08	40.16	40.15
C-13	43.41	43.39	45.85	b	43.15	42.70	43.17	42.72
C-14	56.23	56.14	55.63	49.97**	56.57	56.82	56.65	56.91
C-15	24.30	24.29	24.81	25.85	23.90	23.71	23.92	23.72
C-16	24.64	24.64	24.55	27.18	21.89	23.16	21.90	23.17
C-17	58.83	58.81	50.93	57.55	54.67	54.96	54.70	54.98
C-18	12.87	12.86	13.97	21.08	13.54	13.51	13.55	13.53
C-19	19.41	19.32	19.32	19.31	19.29	19.28	19.37	19.37
C-20	133.95	133.92	134.09	137.94	77.38	78.26	77.40	78.29
C-21	17.83	17.83	23.12	19.10	20.36	21.64	20.36	21.63
C-22	125.71	125.70	129.44	125.31	76.38	76.26	76.37	76.27
C-23	25.88	25.88	26.19	25.96	29.14	29.61	29.14	29.61
C-24	39.16	39.16	39.56	39.11	36.30	36.11	36.31	36.10
C-25	27.68	27.68	27.73	27.73†	28.06	28.37	28.07	28.38
C-26	22.56*	22.56*	22.46*	22.58*	22.35*	22.54*	22.35*	22.52*
C-27	22.62*	22.62*	22.78*	22.60*	22.93*	22.71*	22.94*	22.73*
Acetate		21.44	21.44	21.43	21.44	21.43		
		170.54	170.54	170.55	170.58	170.57		

[a] Data obtained at 125 MHz at 22°C in 20–80 mM $CDCl_3$ solution and referenced to the $CDCl_3$ signal at 77.0 ppm. Assignments marked by †, ††, *, or ** may be interchanged.
[b] Not measured.

temperature for 24 h. Water (20 ml) was added, and the resulting mixture was extracted with ether (3 × 100 ml), dried over anhydrous sodium sulfate, and evaporated to dryness. The residue was subjected to silica gel MPLC (50 × 2 cm) using 5% ethyl acetate in hexane as the eluting solvent. Fractions 9–15 were combined and evaporated to give crude **2a** (850 mg; 96%), which was subjected in 50–100 mg portions to semipreparative Ag^+-HPLC (solvent 1.5% acetone in hexane). The elution of the components was followed by UV absorbance at 210 nm and by analytical Ag^+-HPLC of the fractions. Under these conditions, the $\Delta^{5,20(22)E}$ isomer **2a** was eluted at ~22 min, preceded by the $\Delta^{5,20(22)Z}$ isomer **2b** at 8–12 min and their 17α epimers **2c** (t_R 7–8 min) and **2d** (t_R 11 min).

Characterization of **2a**: mp, 124–125°C (lit. [20] 124.5 ± 0.5°C; lit. [9] 123–125°C; lit. [21] 123–124°C); single component on analytical Ag^+-HPLC (250 × 4.6 mm; solvent, 3% acetone in hexane; t_R 19.3 min); single component on GC-MS (t_R 53.1 min), *m/z* 366 (100, M-CH_3COOH), 351 (10, M-CH_3COOH-CH_3), 313 (2), 253 (10), 240 (4), 228 (27), 216 (16), 211 (11), 145 (17), 107 (11), 95 (20), 81 (26).

Characterization of **2b** (80% purity by ^{1}H NMR): ^{1}H and ^{13}C NMR, Tables 1 and 2.

Characterization of **2c** (80% purity by ^{1}H NMR): ^{1}H and ^{13}C NMR, Tables 1 and 2.

Characterization of **2d** (as a 10:3:3:1 mixture of **2b**: **2a**: **2d**: **2c**): ^{1}H NMR († denotes ± 0.003 ppm precision) δ 5.181† (m, H-22), 2.807 (dd, 9.2, 3.2 Hz, H-17β), 2.030† (br dtd, 17, 5, 2 Hz, H-7β), 2.02 (m, H-23), 1.92 (m, H-23), 1.903† (br tdd, 12, 10.5, 2.5 Hz, H-16β), 1.757† (m, H-15α), 1.664 (q, 1.3 Hz, H-21), 1.630† (dddd, 13, 12, 7, 3 Hz, H-16α), 1.588† (br dd, 17, 11 Hz, H-7α), 1.464† (qd, ~10.5, 5 Hz, H-8β), 1.457† (br dt, 12.6, 3.5 Hz, H-12β), 1.300† (m, H-15β), 1.254† (td, ~13, 5 Hz, H-12α), 1.227† (ddd, 12.8, 10.5, 6.4 Hz, H-14α), 1.022 (s, H-19), 0.941† (td, 12, 6.2 Hz, H-9α), 0.848 (d, 0.6 Hz, H-18); ^{13}C NMR, δ 53.7 (C-14), 50.1 (C-9), 49.3 (C-17), 34.2 (C-12), 32.5 (C-7, C-8), 26.5 (C-15), 25.4 (C-16), 23.1 (C-21), 21.2 (C-18), 19.3 (C-19).

2.4. (20R,22R)-Cholest-5-ene-3β,20,22-triol 3-acetate (**3a**) and (20S,22S)-cholest-5-ene-3β,20,22-triol 3-acetate (**3b**)

To AD-mix-β (7 g) in a mixture of *tert*-butanol (20 ml) and water (20 ml) was added methanesulfonamide (30 mg) and the resulting mixture was cooled to 0°C. The $\Delta^{5,20(22)E}$ diene **2a** (100 mg; 0.23 mmol) in *tert*-butanol (3 ml) was added. Then, *tert*-butanol (2 ml) and water (5 ml) were added and the mixture was kept at 4°C for 24 h. After the disappearance of **2a** (as judged by TLC), sodium sulfite (7 g) was added, and, after stirring for 1 h at room temperature, the mixture was extracted with chloroform (4 × 50 ml). The combined extracts were washed once with brine (20 ml), dried over anhydrous sodium sulfate, and evaporated to dryness. The residue was subjected to silica gel MPLC (50 × 1 cm; solvent, 10% ethyl acetate in hexane). Fractions 10–22 were combined and evaporated to dryness to give, as judged by normal phase HPLC, Ag^+-HPLC, and ^{1}H NMR, an ~1:1 mixture (72 mg; 67%) of **3a** and **3b**.[†] Sterols **3a** and **3b** were incompletely separated on normal phase HPLC (solvent, 3% acetone in hexane; t_R 52.3 min and 54.8 min, respectively) but baseline resolved on analytical Ag^+-HPLC (300 × 3.2 mm; solvent, 10% acetone in hexane; t_R 16.8 min for **3a** and 17.9 min for **3b**). Accordingly, **3a** and **3b** were separated by semipreparative Ag^+-HPLC (250 × 10 mm; solvent, 7.5% acetone in hexane; t_R 47.6 min for **3a** and 52.6 min **3b**).[‡] Fifteen injections [5–7 mg each, dissolved in the mobile phase (500 μl)] furnished **3a** (34 mg) and **3b** (32 mg).

Characterization of the 20*R*,22*R* isomer **3a**: mp, 196–197°C (lit. [9] 192–194°C); single component on analytical Ag^+-HPLC (250 × 4.6 mm; solvent, 9.1% acetone in hexane; t_R 16.6 min); MS, *m/z* 424 (2, M-2H_2O), 400 (1, M-CH_3COOH), 382 (61, M-H_2O-CH_3COOH), 367 (6, M-H_2O-CH_3COOH-CH_3), 364 (15, M-2H_2O-CH_3COOH), 359 (52, M-HOCH$(CH_2)_2$CH$(CH_3)_2$), 349 (6), 341 (13, 359-H_2O), 299 (100, 359-CH_3COOH), 281 (27, 359-CH_3COOH-H_2O), 255 (19, M-SC-CH_3COOH), 159 (38); single major component (99.8%; t_R 82.6 min)[§] by GC-MS of the TMS derivative, *m/z* 517 (6, M-CH_3), 516 (9, M-CH_3-1), 501 (20), 359 (69, M-TMSOCH$(CH_2)_2$CH$(CH_3)_2$), 341 (12, 359-H_2O), 299 (74, 359-CH_3COOH), 281 (25, 359-CH_3COOH-H_2O), 255 (17, M-SC-CH_3COOH), 173 (100, TMSOCH$(CH_2)_2$CH$CH_3)_2$), 83 (54), 73 (73, TMS); ^{1}H and ^{13}C NMR, Tables 1 and 2.

Characterization of the 20*S*,22*S* isomer **3b**: glassy solid; single component on analytical Ag^+-HPLC (250 × 4.6 mm; solvent, 9.1% acetone in hexane; t_R 17.6 min); MS, 424 (2, M-2H_2O), 382 (14, M-CH_3COOH-H_2O), 364 (9, M-CH_3COOH-2H_2O), 359 (31, M-HOCH$(CH_2)_2$CH$(CH_3)_2$), 341 (8, 359-H_2O), 299 (100, 359-CH_3COOH), 281 (25, 359-CH_3COOH-H_2O), 255 (15, M-SC-CH_3COOH); single major component (99.5%; t_R 77.1 min)[§] by GC-MS of the TMS derivative, *m/z* 517 (4, M-CH_3), 516 (6, M-CH_3-1), 501 (13), 359 (62, M-TMSOCH$(CH_2)_2$CH$(CH_3)_2$), 341 (12, 359-H_2O), 299 (84, 359-CH_3COOH), 281 (22, 359-CH_3COOH-H_2O), 255 (15, M-SC-CH_3COOH), 173 (100, TMSOCH$(CH_2)_2$ CH$(CH_3)_2$), 83 (54), 73 (81, TMS); ^{1}H and ^{13}C NMR, Tables 1 and 2.

2.5. (20R,22R)-Cholest-5-ene-3β,20,22-triol (**4a**) and (20S,22S)-cholest-5-ene-3β,20,22-triol (**4b**)

The 20*R*,22*R* isomer **3a** (13 mg) was heated with 15% KOH in 95% ethanol (2 ml) for 2 h at 70°C. After the addition of water (2 ml), the mixture was extracted with methylene chloride (3 × 8 ml), and the combined extracts were washed once with brine (4 ml), dried over anhydrous sodium sulfate, and evaporated to dryness. The residue was applied to a silica gel column (5 × 0.5 cm), and, after washing the column with methylene chloride (20 ml) to remove a nonpolar yellowish impurity, 2-propanol was used to elute the triol. Recrystallization from acetone-hexane gave **4a** as a white solid (10 mg; 84%): mp, 176–178°C (lit. [8] 178–180°C; lit. [12] 179–180°C, lit. [22] 175–178°C); single component on TLC (solvent, 50% acetone in hexane; R_f 0.9); single component on normal phase HPLC (solvent, 9.1% acetone in hexane; t_R 22.3 min); MS, *m/z* 400 (6, M-H_2O), 382 (9, M-2H_2O), 367 (4, M-2H_2O-CH_3), 349 (3, M-3H_2O-CH_3), 317 (100, M-HOCH$(CH_2)_2$CH$(CH_3)_2$), 299 (56, 317-H_2O), 281 (12, 317-2H_2O), 271 (7), 255 (16, M-SC-H_2O), 213 (10), 159 (32), 145 (37); single major component (98.5%; t_R 67.2 min)[§] by GC-MS of the TMS derivative, *m/z* 546 (15, M-CH_3-1), 531 (20), 473 (5), 389 (96, M-TMSOCH$(CH_2)_2$CH$(CH_3)_2$), 371 (12), 370 (11), 299 (58, 389-TMSOH), 281 (18), 255 (14, M-SC-TMSOH), 173 (100, TMSOCH$(CH_2)_2$CH$(CH_3)_2$), 129 (41), 83 (43), 73 (TMS); ^{1}H and ^{13}C NMR, Tables 1 and 2.

Saponification of **3b** (20 mg) and workup (as described above for **3a**) gave **4b** (15 mg; 82%): mp, 168–170°C (lit. [8] 169–171°C); single component on TLC (solvent, 50% acetone in hexane; R_f 0.9) and on normal phase HPLC

[†] When AD-mix-α [17] was used with the same reaction conditions and workup, analyses of the product by normal phase HPLC, Ag^+-HPLC and ^{1}H NMR showed a 1:99 mixture of **3a** and **3b**.

[‡] Compound **3a** can also be isolated by repeated crystallization of the mixture of **3a** and **3b**. An ~1:1 mixture (41 mg) of **3a** and **3b** was recrystallized from 5% acetone in hexane to give **3a**, 95% purity. A second recrystallization gave **3a** (15 mg), 99% purity (as judged by Ag^+-HPLC and ^{1}H NMR).

[§] Minor components with mass spectra compatible with the acetate or TMS ether of pregnenolone were observed in GC-MS analyses of **3a** [0.2%; t_R 19.4 min; *m/z* 298 (100, M-CH_3COOH)], **3b** [0.5%; t_R 19.5 min; *m/z* 298 (100, M-CH_3COOH)], **4a** [1.5%; t_R of 15.8 min; 388 (34, M^+), 373 (9, M-CH_3), 332 (18), 298 (33, M-TMSOH), 283 (16, M-TMSOH-CH_3), 259 (25), 241 (9), 159 (11), 145 (15), 129 (100), 75 (42), 73 (60, TMS)], and **4b** [two minor components of 0.5% each; t_R 14.2 min and 15.7 min; *m/z* 388 (M^+), 298 (M-TMSOH), 283 (M-TMSOH-CH_3), 259, 129, 73]. The minor components in **4b** may represent a pair of C-17 epimers. ^{1}H NMR analysis of **4a** and **4b** indicated no signals for pregnenolone at a detection limit of 0.1%.

(solvent, 9.1% acetone in hexane; t_R 22.9 min); MS, *m/z* 400 (6, M-H_2O), 382 (9, M-2H_2O), 367 (4, M-2H_2O-CH_3), 349 (3, M-3H_2O-CH_3), 317 (100, M-HOCH$(CH_2)_2$ CH$(CH_3)_2$), 299 (56, 317-H_2O), 281 (13, 317-2H_2O), 271 (7), 255 (14, M-SC-H_2O), 213 (9), 159 (32), 145 (34); single major component (98%; t_R 60.9 min)[§] by GC-MS of the TMS derivative, *m/z* 546 (10, M-CH_3-1), 531 (14), 473 (4), 389 (87, M-TMSOCH$(CH_2)_2$CH$(CH_3)_2$), 371 (10), 370 (8), 299 (52, 389-TMSOH), 281 (16), 255 (12, M-SC-TMSOH), 173 (97, TMSOCH$(CH_2)_2$CH$(CH_3)_2$), 129 (41), 83 (41), 73 (100, TMS); ^{1}H and ^{13}C NMR, Tables 1 and 2.

2.6. NOE results

Difference spectra were acquired on nondegassed samples in the usual manner by the irradiation of a single line of a multiplet at low power for 2 s, followed by a 90° read pulse. Enhancements were estimated in difference spectra by comparison of positive signal intensities with the integral of the negative irradiated signal (set at −100%). Enhancements for overlapped or weak signals were estimated approximately (∼), and signals showing coupling to the irradiated resonance were disregarded. The following NOE enhancements were observed (H-23a and H-24a denote the upfield C-23 and C-24 protons, respectively): **1**, irradiation of H-22 [Fig. 1A]: H-16β (4%), H-24 (1%); irradiation of H-21: H-23 (2%), H-16β and H-12β (2%), H-12α (1%), H-18 (1%); **2b**, irradiation of H-22: H-21 (4%), H-24 (2%); irradiation of H-17α: H-23b (5%), H-23a (2%), H-12α (3%), H-14α (5%); irradiation of H-23b: H-17α (4%); irradiation of H-18: H-22 (0.3%), H-16β (2%), H-21 (3%), H-8β (∼2%), H-11β (∼2%), H-15β (2%), H-19 (0.5%); **4a**, irradiation of H-22 [Fig. 1B]: OH (δ 2.26, 3%), OH (δ 1.89, 1%), H-16β (2%), OH (δ 1.64, 1%), H-16α (∼3%), H-17α (∼1%), H-24b (∼2%), H-24a (∼2%); irradiation of H-12β: H-22 (∼1%), H-21 (5%); irradiation of H-16β: H-22 (2%), H-18 (∼1%); irradiation of H-23b: H-16α (∼2%), H-17α (∼1%), H-21 (∼2%).

2.7. Molecular modeling and conformational analysis

Low-energy conformations of sterols **2a**–**d**, **4a**, and **4b** were investigated by varying the side-chain dihedral angles C13-C17-C20-C22, C17-C20-C22-C23, and C20-C22-C23-C24 in PCMODEL using both the MMX and MM3 (1996) force fields. The best conformers are presented in Table 3 and Fig. 2. In $\Delta^{5,20(22)}$ sterols **2a**–**d**, the C20—C22 double bond either roughly eclipses the C17—H17 bond (C13-C17-C20-C22 torsion angle of ca. −90° in 17β-C_8H_{15} sterols or ca. 90° in 17α-C_8H_{15} sterols) or is approximately *anti* to the C17—H17 bond (C13-C17-C20-C22 torsion angles of opposite sign to the preceding values). Molecular modeling results indicated that the *anti* conformer is favored for the $\Delta^{5,20(22)E}$ isomer **2a** (due to steric interactions between the C-18 and C-21 hydrogens in the eclipsed form) and that the eclipsed conformer predominates for the

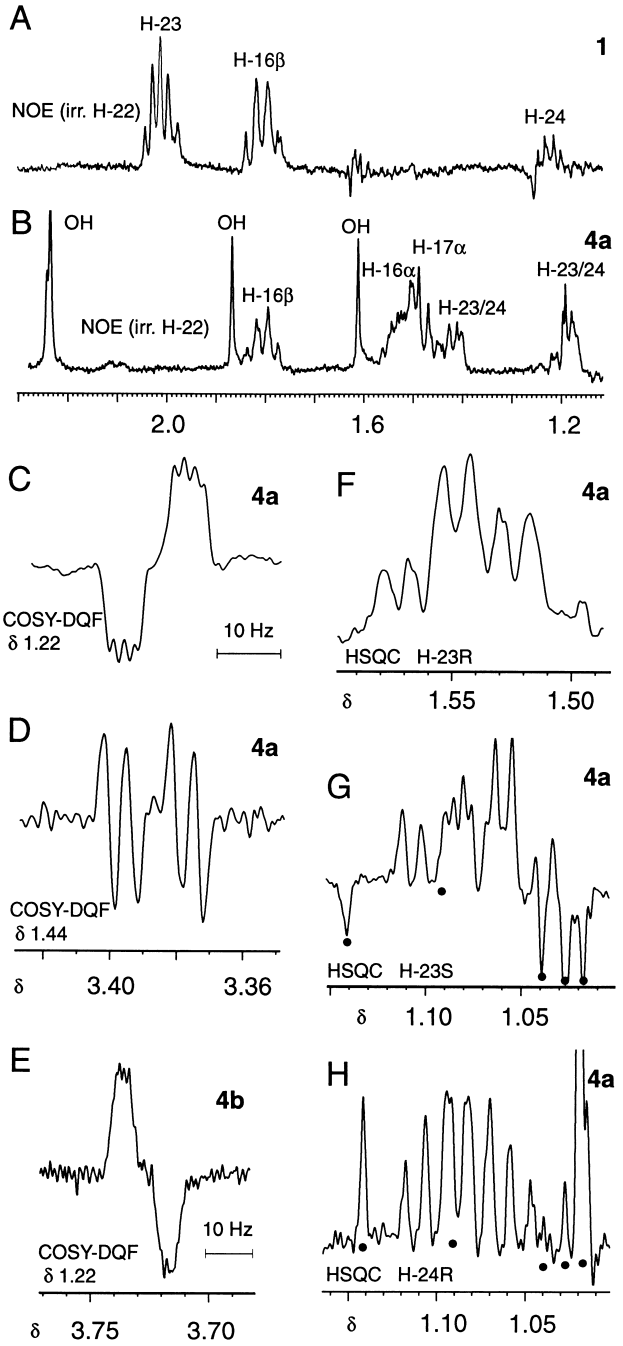

Fig. 1 Representative 500-MHz NMR spectral data used in elucidating side-chain conformations and establishing ^{1}H NMR stereochemical assignments. Panels A and B: NOE difference spectra from irradiation of H-22 of $\Delta^{5,20(22)E}$ diene **1** (A) or triol **4a** (B); 112–160 scans, 0.5 Hz line broadening. Panels C–E: f_2 cross sections through H22-H23 cross peaks in COSY-DQF spectra of **4a** (C and D) and **4b** (E); δ_H 0.8–3.8 spectral window, 1.8-s acquisition time, 200–260 t_1 increments, zero-filled to 8k × 512 points (States-TPPI). Panels F–H: f_2 cross sections of a ^{13}C-coupled HSQC spectrum of **4a**; δ_H 0.7–2.4 and δ_C 19–43 spectral window, 0.9-s acquisition time, 36 t_1 increments, zero-filled to 4k × 32 complex points (States). Closed circles in panels F–H indicate the position of methyl signals, which generate t_1 noise responsible for the positive and negative artifact peaks.

Table 3
Best conformations calculated by molecular mechanics with PCMODEL using the MMX or MM3 force field

	Relative energy[a]		Side-chain torsion angles[b]			Ring D[b]	
	MM3	MMX	C13-C17-C20-C22	C17-C20-C22-C23	C20-C22-C23-C24	$J_{16\alpha-17}$	$J_{16\beta-17}$
2a	0.0	0.0	113	−179	−104	7.2	10.7
	0.2	−0.4	92	179	99	7.5	10.3
	0.7	0.0	−93	−178	−100	7.3	10.5
	1.1	0.6	−93	−179	102	7.2	10.6
2b	0.0	0.0	−99	2	−102	7.2	10.6
	0.1	−0.2	−97	3	121	7.2	10.6
	2.9	2.0	90	−4	−129	7.8	9.9
	2.6	2.4	92	−3	100	7.5	10.3
2c	0.0	0.0	−90	−178	−100	1.1	8.7
	0.5	0.7	−89	180	99	1.2	8.8
	1.1	2.0	112	−178	−101	1.7	9.5
	1.3	1.4	110	−177	111	1.7[c]	9.5[d]
2d	0.0	0.0	111	−2	97	1.7[c]	9.5[d]
	0.0	−0.1	117	1	−98	1.9[c]	9.7[d]
	2.1	0.3	−88	3	116	1.8	9.7
	2.6	1.1	−91	2	−114	1.7	9.6
4a	0.0	0.0	179	63	−177	8.0	9.7
	1.9	2.4	−171	−179	179	8.4	9.4
	1.9	2.5	−177	65	−100	7.9	9.8
4b	0.0	0.0	−145	−61	−178	7.6	10.3
	1.1	1.4	−164	54	168	7.6	10.2
	1.7	2.9	−165	171	178	7.4	10.4

[a] Relative steric energies (kcal/mol) calculated with the MM3 (1996) or MMX force field in PCMODEL 7. The MM3 (MMX) steric energies (kcal/mol) for the best conformers were: 61.5 (45.8) for **2a**, 62.0 (46.5) for **2b**, 63.1 (46.2) for **2c**, 64.2 (47.3) for **2d**, 69.8 (47.3) for **4a**, and 73.1 (50.1) for **4b**. A glycol hydrogen bond was present in some MMX calculations but not in the lowest-energy structures for **4a**.
[b] Values of torsion angles (in degrees) and predicted NMR coupling constants (in Hz) were determined from MM3 structures.
[c] Couplings predicted with MMX: 5.9–6.5 Hz.
[d] Couplings predicted with MMX: 10.0–10.2Hz.

$\Delta^{5,20(22)Z}$ isomer **2b** (due to steric interactions between the C-18 and C-23 hydrogens in the *anti* form). The prevailing conformers of **2a** and **2b**, shown in Fig. 2, are open to attack on the 20-*Re* and 20-*Si* face (giving 20*S*,22*S* and 20*R*,22*S* dihydroxylation products), respectively, and sterically shielded on the opposite face by the C-13 methyl group[¶]. This conformational analysis, which is compatible with NOE results for **2a** and **2b**, provides a basic (albeit oversimplified) model for understanding oxidative addition to the $\Delta^{20(22)}$ bond.

The usual C_8H_{17} sterol side chain is mainly in the extended conformation, in which all backbone C-C-C-C dihedrals are *anti*. The 20*R*,22*R*-dihydroxy substitution in triol **4a** alters the extended conformation by changing the C17-C20-C22-C23 dihedral to +*gauche*, as indicated by molecular mechanics energies (Table 3) and NOE results [notably strong enhancements of H-16α and H-16β from irradiation of H-22, as shown in Fig. 1B]. These results also suggest that no other conformers are significantly populated. The +*gauche* dihedral in the major conformer of **4a** is analogous to angles observed in the 22*R* isomer of 1α,22,25-trihydroxy vitamin D [23] and in the crystal structure of 20-hydroxy ecdysone [24], another 20*R*,22*R* glycol. Molecular modeling also predicted a single major conformer (~80% population) for the 20*S*,22*S* triol **4b** with a −*gauche* C17-C20-C22-C23 dihedral and a distorted *anti* C13-C17-C20-C22 dihedral. The C20-C22-C23-C24 dihedral was *anti* in all low-energy conformers of **4a** and **4b**.

Molecular modeling was done in PCMODEL with the classical MMX and recently implemented MM3 (1996) force fields as well as with the original MM3 (94) package and a version of MM2 from Chem3D. Relative energies varied somewhat among the force fields and were sensitive to the location of the hydroxyl hydrogen, but MMX, MM3 (1996), and MM3 (94) were fundamentally in agreement regarding the low-energy conformers. However, MM3 (1996) and MM3 (94) appeared to be less prone than MMX to fall into artifactual energy minima. Also, MMX predicted ring D of $\Delta^{5,20(22)Z}$ diene **2d** to be a 14α-envelope, whereas the MM3 conformation (intermediate between a 13β-envelope and 13β,14α-half chair) gave predicted $J_{16\text{-}17}$ coupling constants (Table 3) compatible with observed values. Even when started with the MM3 coordinates, MMX converged to a 14α-envelope. The MM3 (94) program gave ring D geometries very similar to those of MM3 in PCMODEL

[¶] Early force-field calculations showing **2a** to be mainly in the eclipsed conformation were used to rationalize the catalytic addition of hydrogen from the 20-*Si* (α) face of the $\Delta^{20(22)}$ bond [20], but this addition was later noted to involve double-bond isomerization followed by hydrogenation [19].

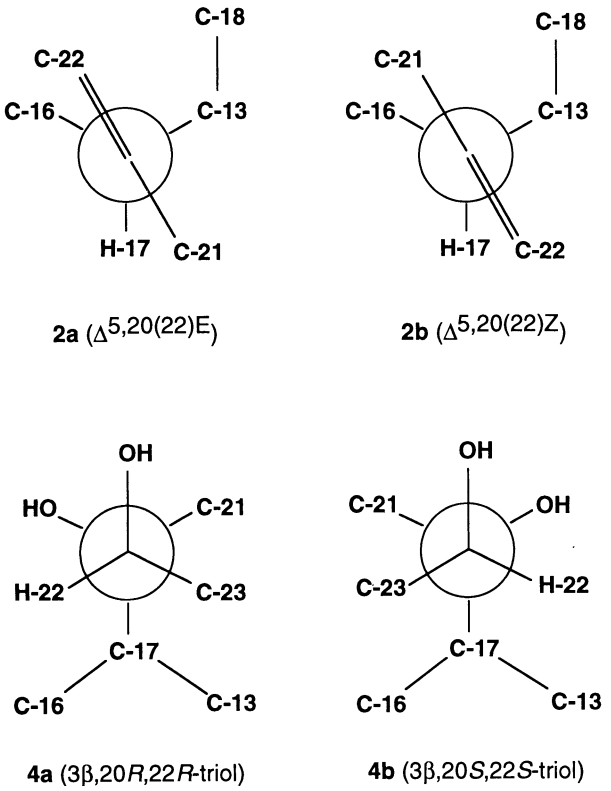

Fig. 2. Newman projections of the best conformers of $\Delta^{5,20(22)}$ dienes **2a** and **2b** looking down the C20-C17 bond and the best conformers of 3β,20,22-triols **4a** and **4b** looking down the C22-C20 bond.

from either MMX or MM3 coordinates, whereas minimizations in Chem3D essentially retained the initial MMX or MM3 geometry for ring D regardless of which starting input coordinates were used. These observations indicate advantages of the more complex MM3 force field over MMX and MM2/Chem 3D for modeling ring D and the sterol side chain.

2.8. Structure determinations by NMR

Structures of sterols reported herein were compatible with ^{1}H and ^{13}C NMR, COSYDEC, and HSQC spectral data. The 20*R*,22*R* isomers **3a** and **4a** were distinguished from the 20*S*,22*S* isomers **3b** and **4b** (and other possible stereoisomers) by the reported trends among 20,22-dihydroxysterols for ^{13}C NMR chemical shifts [25] of C-16 and C-21 and ^{1}H NMR chemical shifts [8,9,11,12,25] of H-21 and H-22 (Tables 1 and 2). The $\Delta^{5,20(22)E}$ dienes **2a** and **2c** were distinguished from their $\Delta^{5,20(22)Z}$ isomers **2b** and **2d** by the known [26] *cis* shielding effect of C-23 on C-17 or C-21. Isomers **2a** and **2b** were assigned the 17β-C_8H_{15} stereochemistry by comparison of their ^{1}H and ^{13}C NMR chemical shifts with data reported previously [9,19–21,26,27] for $\Delta^{5,20(22)}$ sterols. The 17α-C_8H_{15} stereochemistry of **2c** and **2d** was based on mechanistic expectation, agreement between observed and predicted coupling constants (Tables 1 and 3), and γ-*gauche* effects of the C-17 substituent on the ^{13}C NMR chemical shifts of C-12, C-14, and C-18 (Table 2).

2.9. NMR signal assignments

^{13}C NMR signals were assigned by chemical shift comparisons [15] with other Δ^5 sterols together with results of DEPT, HSQC, and COSYDEC spectra. Approximate ($\pm$0.003 ppm) ^{1}H chemical shifts were then read directly from the HSQC spectrum, and more accurate values ($\pm$0.001 ppm) were obtained from 1D and COSYDEC spectra. Stereochemical assignments of ^{1}H signals followed from chemical shift comparisons with similar Δ^5 sterols [15], except for the C-16 protons (established from their characteristic peak shape revealed in HSQC spectra) and side-chain protons. Stereochemical assignments of the C-23 protons of triols **4a** and **4b** were based on NOE results and/or comparison of observed coupling constants with those predicted from MM3 structures. The downfield C-23 proton was assigned as pro-*R* based on its irradiation producing an NOE enhancement for H-16α, which is 2.7 Å from H-23*R*, but 4.2 Å from H-23*S* in the prevailing conformer of **4a**. This assignment was confirmed by the agreement of predicted $J_{H22\text{-}H23R}$ and $J_{H22\text{-}H23S}$ values (1.7 and 11.4 Hz) with the active couplings observed in COSY-DQF cross peaks [Fig. 1C, D] and with the H-23*R* and H-23*S* coupling patterns from a coupled [16] HSQC spectrum [Fig. 1F, G]. The resonances of the C-23 and C-24 protons were highly second-order at 500 MHz in 1D and decoupled HSQC spectra owing to the near isochronicity of H-23R with H-24S and of H-23S with H-24R (each pair mutually coupled by ~11 Hz), but some of the ^{13}C satellite signals in coupled HSQC spectra [16] showed markedly diminished second-order effects to give interpretable (albeit distorted) multiplets [Fig. 1F–H]. The upfield C-23 proton of **4b** was assigned similarly as pro-*R* by matching predicted values of $J_{H22\text{-}23R}$ and $J_{H22\text{-}23S}$ (11.6 and 2.1 Hz) to the active coupling observed in the COSY-DQF spectrum [Fig. 1E]. As in other sterols, the C22-C23-C24-C25 dihedral is mainly *anti* in triols **4a** and **4b**, as judged by molecular modeling and by the H-23 and H-24 coupling patterns of **4a** [Fig. 1F–H and Table 1]. By analogy with the downfield shift of H-1α upon 3α-hydroxylation of 5α-cholestane [28], the C-24 proton proximate to oxygen at C-22 will be shifted downfield relative to both its geminal partner and the C-24 protons ($\delta \sim 1.12$) of sterols with a C_8H_{17} side chain. Thus, H-24*S* of **4a** and H-24*R* of **4b** (both proximate to the 22-hydroxyl) were assigned as the downfield C-24 protons. These assignments are compatible with the high degree of strong coupling observed between the C-23 and C-24 protons at 500 MHz.

3. Discussion

Several methods are available for constructing 20,22-dihydroxy derivatives of cholesterol, the most important of

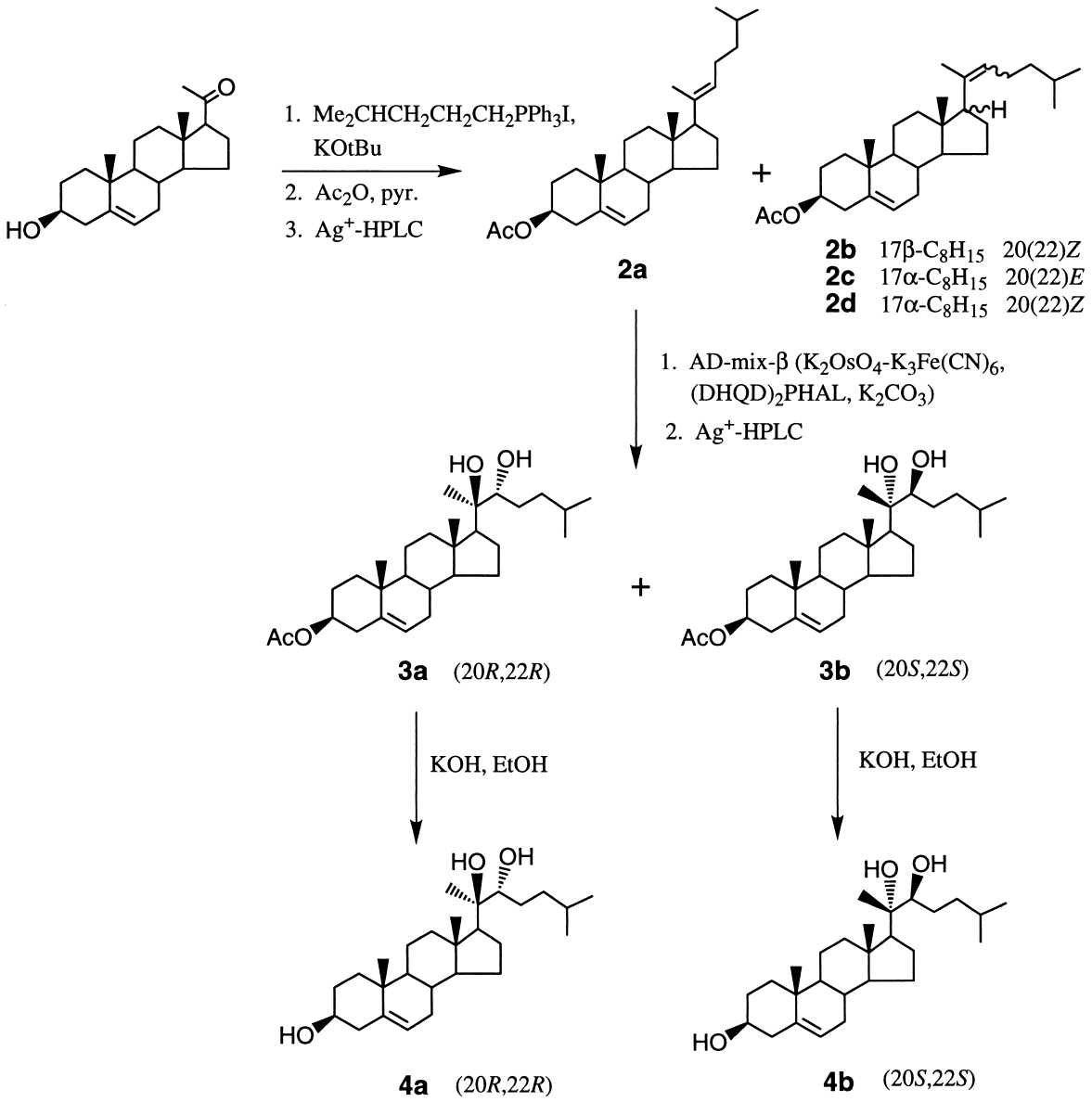

Scheme 1. Synthesis of (20*R*,22*R*)-cholest-5-ene-3*β*,20,22-triol **4a** and its 20*S*,22*S* epimer **4b** from pregnenolone.

which is the natural 20*R*,22*R* isomer **4a**. Reported chemical methods, which include dihydroxylation of $\Delta^{20(22)}$ olefins with osmium tetroxide [9–12,19], Grignard addition to C_{22}-20-hydroxy-22-aldehydes [8–10,12,22,25], epoxidation of allylic 20-hydroxy-C_{23} steroids followed by addition of R_2CuLi [12], epoxidation of $\Delta^{20(22)}$ olefins followed by ring opening [12], and various reductions of 20-hydroxy-22-ketosterols [8,9,10,26], give predominantly unnatural isomers. For example, steric factors direct osmium tetroxide to the back face of the $\Delta^{20(22)E}$ double bond to produce almost exclusively (≥90%) the unnatural 20*S*,22*S* isomer **4b** [9–12,19]. Owing to more favorable side-chain conformations, dihydroxylation of $\Delta^{20(22)Z}$ sterols [9,27] proceeds from the desired 20-*Si* face, but the *Z* geometry furnishes the 22S isomer. These and other [29] efforts to overcome unfavorable diastereoselectivity, together with the design of synthetic strategies around the potential reactivity of the Δ^5 double bond, have resulted in lengthy and inefficient routes to **4a**.

Our synthesis of **4a** (Scheme 1) began with the Wittig reaction of pregnenolone with isohexyltriphenylphosphonium iodide. Early reports of this reaction [19,20] claimed exclusive formation of the $\Delta^{5,20(22)E}$ isomer, but modern analytical methods (Ag^+-HPLC and high-field NMR) revealed 5% of the $\Delta^{5,20(22)Z}$ isomer **2b** and lower levels of the 17α epimers **2c** and **2d**, which evidently arose from partial epimerization of pregnenolone under the alkaline Wittig conditions. Complete removal of these byproducts was essential to avoid the formation of a complex isomeric mixture in the subsequent oxidation step. The addition of osmium tetroxide to $\Delta^{20(22)E}$ sterols has been reported to give mixtures of 20*S*,22*S*: 20*R*,22*R* isomers in a ratio of 9:1

Table 4
Oxidation of $\Delta^{20(22)E}$ sterols with osmium tetroxide.

Reagent	Product ratio 20*S*,22*S*: 20*R*,22*R*
OsO_4, Et_2O, pyr.	9:1[a]
AD-mix-α	99:1[b]
AD-mix-β	1:1[b]

[a] Product ratio by HPLC analysis of oxidations of [20(22)-*E*]-5α-cholest-20(22)-en-3β-ol acetate (Ref. 11), its benzoate analog (Ref. 11), or **2a** (Ref. 12). Isolated products from oxidation of **2a** or its benzoate analog gave ratios of 13:1 (Ref. 9) or 14:1 (Ref. 10).

[b] This work; substrate, [20(22)-*E*]-cholesta-5,20(22)-dien-3β-ol acetate (**2a**).

[11,12], 13:1 [9], or 14:1 [10]. In an attempt to overcome this unfavorable diastereoselectivity, we investigated the use of enantioselective reagents developed by Sharpless et al. [17]. Oxidations were carried out with catalytic amounts of K_2OsO_4 in the presence of $K_3Fe(CN)_6$ as a cooxidant and either [$(DHQ)_2$(PHAL)] (AD-mix-β) or $(DHQD)_2$PHAL (AD-mix-α) as a chiral ligand binding to OsO_4. AD-mix-α enhanced the diastereoselectivity of addition to give a 99:1 ratio of 20*S*,22*S*: 20*R*,22*R* isomers, whereas AD-mix-β led to a mismatch of enantioselectivity with the inherent diastereoselectivity of the sterol geometry to give a favorable 1:1 ratio of isomers **3b** and **3a**. These results are summarized in Table 4. Separation of **3a** and **3b** by semipreparative Ag^+-HPLC followed by saponification furnished the free sterols **4a** and **4b**.

It is noteworthy that the AD-mix-β oxidation reaction proceeded in 67% yield without any protection of the Δ^5 double bond. This favorable regioselectivity, which has been achieved previously for osmium tetroxide oxidation of $\Delta^{5,20(22)E}$ sterols [9–12], led to a remarkably brief synthesis of the natural 20*R*,22*R* isomer **4a**. This synthesis (Scheme 1) consists of four steps, two of which are acetylation and deacetylation reactions. The overall yield of triols **4a** and **4b** were each ca. 15% from pregnenolone. (Triol **4b** can be prepared more efficiently by oxidation with AD-mix-α.) Although two critical separations by semipreparative Ag^+-HPLC are described herein, alternative purification methods may be feasible for work on a larger scale. For example, silica gel- or alumina-$AgNO_3$ MPLC [30] should be sufficient for purifying the $\Delta^{5,20(22)E}$ diene **2a**, and 20,22-diol isomers can be purified by normal-phase HPLC [9,12] or by recrystallization from acetone [10] or acetone-hexane (described herein). The utility of Ag^+-HPLC for resolving the glycol isomers **3a** and **3b** demonstrates that this powerful method has applications beyond the olefinic isomer separations to which it is normally applied [13,14].

The synthetic triols **4a** and **4b** were obtained in high purity as judged by TLC, Ag^+-HPLC, and 500-MHz ^{1}H NMR. Assignments of the stereochemistry at C-20 and C-22 in **3a**, **3b**, **4a**, and **4b** were based upon comparisons of the melting point and NMR data with those reported previously [8,9,12]. Triols **4a** and **4b** and their synthetic precursors were characterized by chromatography, MS, and ^{1}H and ^{13}C NMR (Tables 1 and 2). The high precision of the NMR data should be useful for distinguishing the isomers described herein from the many possible isomeric byproducts that may be formed in syntheses of 3β,20,22-triols. The high precision also revealed interesting differences in long-range effects of the two 20,22-dihydroxy isomers on chemical shifts. For example, ^{1}H NMR signals from the steroid nucleus of the 20*R*,22*R* isomer are shifted slightly downfield relative to those of the 20*S*,22*S* isomer, except for H-1α and protons in ring D. These observations may be attributable to electric field effects arising from differences in orientation of the hydroxyl groups between the two isomers (Fig. 2). Appreciable chemical shift differences were also observed in the side chain, where ^{1}H NMR stereochemical assignments were established by a combination of 2D NMR, NOE results, and molecular modeling. Correlation of conformations predicted by molecular mechanics with NMR data indicated the advantages of MM3 over simpler force fields for modeling ring D and the side chain of sterols. Conformational analysis was also useful in elucidating the structures of the four $\Delta^{5,20(22)}$ diene isomers and in formulating a simple intuitive model for rationalizing the stereochemistry of 20,22-glycols formed by OsO_4 oxidation of $\Delta^{20(22)}$ sterols. However, true understanding of the basis for the observed diastereoselectivities must await realistic modeling of the competing transition-state species.

Acknowledgments

This work was supported in part by grants from the National Institutes of Health (HL-49122) and the Robert A. Welch Foundation (C-583).

References

[1] Burstein S, Middleditch BS, Gut M. Mass spectrometric study of the enzymatic conversion of cholesterol to (22R)-22-hydroxycholesterol, (20R,22R)-20,22-dihydroxycholesterol, and pregnenolone, and of (22R)-22-hydroxycholesterol to the glycol and pregnenolone in bovine adrenocortical preparations. Mode of oxygen incorporation. J Biol Chem 1975;250:9028–37.

[2] Tuckey RC. Cholesterol side-chain cleavage by mitochondria from the human placenta. Studies using hydroxycholesterols as substrates. J Steroid Biochem Mol Biol 1992;42:883–90.

[3] Sugano S, Miura R, Morishima N. Identification of intermediates in the conversion of cholesterol to pregnenolone with a reconstituted cytochrome P-450_{scc} system: Accumulation of the intermediate modulated by adrenodoxin level. J Biochem 1996;120:780–7.

[4] Dixon R, Furutachi T, Lieberman S. The isolation of crystalline 22R-hydroxycholesterol and 20α,22R-dihydroxycholesterol from bovine adrenals. Biochem Biophys Res Commun 1970;40:161–5.

[5] Janowski BA, Willy PJ, Devi TR, Falck JR, Mangelsdorf DJ. An oxysterol signalling pathway mediated by the nuclear receptor LXRα. Nature 1996;383:728–31.

[6] Forman BM, Ruan B, Chen J, Schroepfer GJ Jr, Evans RM. The orphan nuclear receptor LXRα is positively and negatively regulated by distinct products of mevalonate metabolism. Proc Natl Acad Sci USA 1997;94:10588–93.
[7] Tuckey RC, Cameron KJ. Human placental cholesterol side-chain cleavage: Enzymatic synthesis of (22R)-20α,22-dihydroxycholesterol. Steroids 1993;58:230–3.
[8] Chaudhuri NK, Nickolson R, Kimball H, Gut M. The synthesis and stereochemistry of (22R)-20α,22- and (22S)-20α,22-dihydroxycholesterol. Steroids 1970;15:525–39.
[9] Byon CY, Gut M. Stereospecific synthesis of the four 20,22-epoxycholesterols and of (Z)-20(22)-dehydrocholesterol. J Org Chem 1976; 41:3716–22.
[10] Koreeda M, Koizumi N, Teicher BA. Stereochemically controlled syntheses of 20,22-epoxycholesterols. Tetrahedron Lett 1976;4565–8.
[11] Bannai K, Morisaki M, Ikekawa N. Studies on steroids. Part 37. Synthesis of four stereoisomers of 20,22-epoxycholesterol. J Chem Soc, Perkin Trans 1 1976;2116–20.
[12] Morisaki M, Sato S, Ikekawa N. Studies on steroids. XLV. Synthesis of four stereoisomers of 20,22-dihydroxycholesterol. Chem Pharm Bull 1977;25:2576–83.
[13] Ruan B, Shey J, Gerst N, Wilson WK, Schroepfer GJ Jr. Silver ion high pressure liquid chromatography provides unprecedented separation of sterols: Application to the enzymatic formation of cholesta-5,8-dien-3β-ol. Proc Natl Acad Sci USA 1996;93:11603–8.
[14] Ruan B, Gerst N, Emmons GT, Shey J, Schroepfer GJ Jr. Sterol synthesis. A timely look at the capabilities of conventional and silver ion high performance liquid chromatography for the separation of C_{27} sterols related to cholesterol biosynthesis. J Lipid Res 1997;38:2615–26.
[15] Wilson WK, Sumpter RM, Warren JJ, Rogers PS, Ruan B, Schroepfer GJ Jr. Analysis of unsaturated C_{27} sterols by nuclear magnetic resonance spectroscopy. J Lipid Res 1996;37:1529–55.
[16] Simova S. Applications of HSQC to the measurement of homonuclear coupling constants, J(H,H). Magn Reson Chem 1998;36:505–10.
[17] Sharpless KB, Amberg W, Bennani YL, Crispino, GA, Hartung J, Jeong K-S, Kwong H-L, Morikawa K, Wang Z-M, Xu D, Zhang X-L. The osmium-catalyzed asymmetric dihydroxylation: A new ligand class and a process improvement. J Org Chem 1992;57:2768–71.
[18] Rydon HN. Akyl iodides: Neopentyl iodide and iodocyclohexane. Org Synth Coll Vol 1988;6:830–2.
[19] Schow SR, McMorris TC. Utility of the Wittig reaction for the construction of side chains of steroids starting with pregnenolone. J Org Chem 1979;44:3760–5.
[20] Schmit JP, Piraux M, Pilette JF. Application of the Wittig reaction to the synthesis of steroidal side chains. Possibility of 3β-phenoxy formation as a secondary reaction. J Org Chem 1975;40:1586–8.
[21] Nes WR, Varkey TE, Crump DR, Gut M. (Z)-17(20)-Dehydrocholesterol. A new sterol with C-21 and C-22 spatially fixed. J Org Chem 1976;41:3429–33.
[22] Sydykov ZhS, Segal GM. Partial synthesis of 20(R),22(R)-Δ^5-cholestene-3β,20,22-triol. Izv Akad Nauk SSSR, Ser Khim 1977;161–164.
[23] Iguchi T, Yoshida M, Ikekawa N. Synthesis and biological activities of 22-hydroxy and 22-methoxy derivatives of 1α,25-dihydroxyvitamin D_3: Importance of side chain conformation for biological activities. Bioorg Chem 1989;17:294–307.
[24] Duax WL, Griffin JF, Rohrer DC, Weeks CM. Conformational analysis of sterols: Comparison of X-ray crystallographic observations with data from other sources. Lipids 1980;15:783–92.
[25] Hikino H, Okuyama T, Arihara S, Hikino Y, Takemoto T, Mori H, Shibata K. Shidasterone, an insect metamorphosing substance from *Blechnum niponicum*: structure. Chem Pharm Bull 1975;23:1458–79.
[26] Anderson WG, Byon CY, Gut M, Bissett FH. ^{13}C NMR studies of the four 20,22-epoxycholesterols and the two 20(22)-dehydrocholesterols. Tetrahedron Lett 1976;2193–6.
[27] Koreeda M, Koizumi N, Teicher, BA. Stereospecific synthesis of (Z)-20(22)-didehydrocholesterol. J Chem Soc Chem Commun 1976; 1035–6.
[28] Schneider H-J, Buchheit U, Becker N, Schmidt G, Siehl U. ^{1}H NMR analyses, shielding mechanisms, coupling constants, and conformations in steroids bearing halogen, hydroxy, oxo groups, and double bonds. J Am Chem Soc 1985;107:7027–39.
[29] Kyler KS, Watt DS. Partial synthesis of (20R,22R)-20,22-dihydroxycholesterol. J Org Chem 1981;46:5182–8.
[30] Pascal RA Jr, Farris CL, Schroepfer GJ Jr. Sterol synthesis: medium-pressure chromatography of C_{27} sterol precursors of cholesterol on alumina-silver nitrate columns. Anal Biochem 1980;101:15–22.